molecular pharmaceutics

Article

Near infrared photoimmunotherapy with combined exposure of external and interstitial light sources

Yasuhiro Maruoka, Tadanobu Nagaya, Kazuhide Sato, Fusa Ogata, Shuhei Okuyama, Peter L Choyke, and Hisataka Kobayashi

Mol. Pharmaceutics, **Just Accepted Manuscript** • DOI: 10.1021/acs.molpharmaceut.8b00002 • Publication Date (Web): 16 Feb 2018

Just Accepted

ACS Publications

Molecular Pharmaceutics is published by the American Chemical Society. 1155 Sixteenth Street N.W., Washington, DC 20036

Near infrared photoimmunotherapy with combined exposure of external and interstitial light sources.

Yasuhiro Maruoka[1], Tadanobu Nagaya[1], Kazuhide Sato[1], Fusa Ogata[1], Shuhei Okuyama[1], Peter L. Choyke[1], Hisataka Kobayashi[1]

[1]Molecular Imaging Program, Center for Cancer Research, National Cancer Institute, NIH, Bethesda, MD, 20892, USA

Corresponding author:

Hisataka Kobayashi, M.D., Ph.D.

Molecular Imaging Program, Center for Cancer Research, National Cancer Institute, NIH, 10 Center Drive, Bethesda, MD, 20892, USA

Tel: 301-435-4086

Fax: 301-402-3191

E-mail: kobayash@mail.nih.gov

ABSTRACT

Near infrared photoimmunotherapy (NIR-PIT) is a new target-cell specific cancer treatment that induces highly selective necrotic/immunogenic cell death after systemic administration of a photoabsorber antibody conjugate and subsequent NIR light exposure. However, the depth of NIR light penetration in tissue (approximately 2 centimeters) with external light sources, limits the therapeutic effects of NIR-PIT. Interstitial light exposure using cylindrical diffusing optical fibers can overcome this limitation. The purpose in this study was to compare three NIR light delivery methods for treating tumors with NIR-PIT using a NIR laser system at an identical light energy; external exposure alone, interstitial exposure alone, and the combination. Panitumumab conjugated with the photoabsorber, IRDye-700DX (pan-IR700) was intravenously administered to mice with A431-luc xenografts which are epithelial growth factor receptor (EGFR) positive. One and two days later, NIR light was administered to the tumors using one of three methods. Interstitial exposure alone and in combination with external sources showed the greatest decrease in bioluminescence signal intensity. Additionally, the combination of external and interstitial NIR light exposure showed significantly greater tumor size reduction and prolonged survival after NIR-PIT compared to external exposure alone. This result suggested that the

combination of external and interstitial NIR light exposure was more effective than externally applied light alone. Although external exposure is the least invasive means of delivering light, the combination of external and interstitial exposures produces superior therapeutic efficacy in tumors greater than 2 cm in depth from the tissue surface.

Keywords: near infrared photoimmunotherapy, light delivery method, combination, external exposure, interstitial exposure

INTRODUCTION

Near infrared photoimmunotherapy (NIR-PIT) is a newly-developed cancer treatment that induces highly selective cell death to targeted tumor cells. It uses a monoclonal antibody conjugated with a photoabsorber, silica-phthalocyanine (IRDye700DX: IR700) dye [1] which is systemically injected. Following exposure to NIR light at 690 nm wavelength, cells binding the conjugate will be acutely killed by a process of membrane damage leading to cell blebbing and rupture. Unlike other cancer therapies, which commonly lead to the apoptotic cell death [2, 3], NIR-PIT induces highly specific necrotic/immunogenic cell death in tumors with minimal or no adverse effects in normal tissue [1, 4-7]. Based on promising preclinical results a Phase I/ Π trial of NIR-PIT was initiated using cetuximab-IR700 in patients with inoperable head and neck cancer in 2015 (https://clinicaltrials.gov/ct2/show/ NCT02422979). Cetuximab targets epidermal growth factor receptor (EGFR) which is usually overexpressed in head and neck cancers.

The 690 nm peak absorbance of IR700 provides some advantage over visible light because it allows deeper light penetration. While NIR-PIT effects can be observed to several centimeters beneath the skin surface this severely limits the number of tumors that can be treated in this manner [8]. To overcome this limitations various strategies

have been proposed including light delivery via catheters, endoscopes, or needles etc. The most universal of these is the placement of interstitial optical fibers with distal optical diffusers. This concept was first employed in photodynamic therapy (PDT) which uses a porphyrin based photosensitizer [9] and has been applied in prostate cancer [10], tongue base carcinoma [11], and cholangiocarcinoma [12], among others.

However, in the case of NIR-PIT, it remains unclear whether surface irradiation alone, interstitial irradiation or a combination is the preferred approach. In this study, we compare the *in vivo* therapeutic efficacy of NIR-PIT using external exposure alone, interstitial exposure alone, and a combination of both external and interstitial exposures as the optimal NIR light delivery method.

MATERIALS AND METHODS

Cell culture

A431-luc cells expressing human epidermal growth factor receptor 1 (EGFR) with the gene encoding firefly luciferase were cultured in RPMI1640 supplemented with 10% FBS and 1% penicillin-streptomycin in tissue culture flasks in a humidified incubator at 37ºC in an atmosphere of 95% air and 5% carbon dioxide.

Reagents

Water soluble, silica-phthalocyanine derivative, IRDye700DX NHS ester was obtained from LI-COR Bioscience (Lincoln, NE, USA). Panitumumab, a fully humanized IgG2 monoclonal antibodies against EGFR, was purchased from Amgen (Thousand Oaks, CA, USA). All other chemicals were of reagent grade.

Synthesis of IR700-conjugated panitumumab

Panitumumab (1 mg, 6.8 nmol) was incubated with IR700 (66.9 μg, 34.2 nmol, 10 mmol/L in DMSO) and 0.1 mol/L Na_2HPO_4 (pH 8.5) at room temperature for 1 h. The mixture was purified with a gel filtration column (Sephadex G 25 column, PD-10, GE Healthcare, Piscataway, NJ, USA). The protein concentration was determined with Coomassie Plus protein assay kit (Thermo Fisher Scientific Inc, Rockford, IL, USA) by measurement of the absorption at 595 nm with spectroscopy (8453 Value System; Agilent Technologies, Santa Clara, CA, USA). We abbreviate the panitumumab-IR700-conjugate as pan-IR700.

Animal model

All procedures were performed in compliance with the Guide for the Care and Use of Laboratory Animals and approved by the local Animal Care and Use Committee. Female homozygote athymic nude mice aged 6- to 8-weeks were used (Charles River National Cancer Institute Frederick). A431-luc cells (2×10^6 in phosphate-buffered

saline) were subcutaneously injected in the dorsi of the mice under inhaled isoflurane anesthesia.

NIR-PIT

Seven days after cell inoculation, mice with tumors reaching approximately 100 mm^3 in volume were selected for further experiments. Tumor volumes were calculated from the greatest longitudinal diameter (length) and the greatest transverse diameter (width) using the following formula; tumor volume = length × $width^2$ × 0.5, based on caliper measurements. Tumor volumes (up to 2,000 mm^3) were measured until the mice were euthanized in compliance with humane endpoints. All mice in this study were divided randomly into 4 experimental groups for the following treatments: (1) no treatment (control); (2) intravenous injection of 100 μg pan-IR700 followed by external NIR light exposure using a laser system (BWF5-690-8-600-0.37; B & W TEK INC., Newark, DE, USA) with a 10mm beam collimator at 50 J/cm^2 on day 0 and 100 J/cm^2 on day 1 (external exposure alone); (3) intravenous injection of 100 μg pan-IR700 followed by interstitial NIR light exposure using the laser system with a cylindrical diffusing fiber at 50 J/cm on day 0 and 100 J/cm on day 1 (interstitial exposure alone); and (4) intravenous injection of 100 μg pan-IR700 followed by combination with external NIR light exposure (25 J/cm^2 on day 0 and 50 J/cm^2 on day 1) and interstitial

laser NIR light exposure (25 J/cm on day 0 and 50 J/cm on day 1) at the same time (combined exposure). During external light exposure, NIR light was delivered from the top side of the tumor. Interstitial exposure was performed with a cylindrical diffusing fiber with a diameter of 0.98 mm and a 30 mm irradiation length (Ecublens, Switzerland) which was percutaneously inserted into the targeted tumors using an 18G needle with a translucent catheter (SR-OX1864CA; TERUMO, Tokyo, Japan). Light sources used in external exposure and interstitial exposure are respectively classified into planar sources and linear sources. Thus, in this study, the light dose administered with external exposure was considered planar and therefore was measured in units of energy per surface area (J/cm^2) whereas interstitial fibers were assumed to be linear and therefore based on energy per unit length (J/cm). Previously [13], it has been reported that the light dose in J/cm is almost equivalent to J/cm^2 within the small dimensions used here. In order to deliver the same light dose with external or interstitial exposures, the time of exposure was carefully adjusted.

Analysis of IR700 fluorescence imaging and bioluminescence imaging (BLI)

IR700 fluorescence images were obtained with the Pearl Imager (LI-COR Bioscience) using the 700 nm fluorescence channel. Regions of interest (ROI) were placed on the tumor and the mean fluorescence intensity was calculated for each ROI.

Percent Target-to-background ratio (TBR) was calculated from fluorescence intensities (FI) of tumors and background using the following formula; (FI tumor) – (FI background) / (FI background) x 100. Scans of IR700 fluorescence images were performed before and after NIR light exposure on day 0 to day 3 (Figure 2A).

To obtain BLI, D-luciferin (15 mg/mL, 200 μL) was intraperitoneally injected 5 minutes before image acquisition. Luciferase activity was analyzed with a Photon Imager (Biospace Lab, Paris, France) in relative light units (RLU). Regions of interest (ROI) were placed over the entire tumor. The counts per minute of RLU were calculated using M3 Vision Software (Biospace Lab), and converted to the percentage change in RLU (%RLU) by comparing with RLU prior to treatment. BLI was performed on day 0 to day 6 (Figure 3A).

Statistical Analysis

Quantitative data were expressed as means ± SEM. For multiple comparisons (≥ 3 groups), a one-way analysis of variance followed by the Tukey-Kramer test was used. The cumulative probability of survival was analyzed by the Kaplan-Meier survival curve analysis, and the results were compared with the Log-rank test. The paired *t*-tests were used to compare the parameters before and after NIR light exposure in PIT. Statistical analysis was performed with JMP 13 software (SAS Institute, Cary, NC). A *p*

value of less than 0.05 was considered significant.

RESULTS

Overview of light delivery methods and changes in IR700 FI after NIR-PIT

The characteristics of external and interstitial exposure as NIR light delivery methods in NIR-PIT are shown in Figure 1. NIR laser light used in this study has a narrow bandwidth (685–695 nm) and delivers coherent light making light delivery more efficient [14]. Fluorescence images were obtained before and after NIR light exposure up to day 3 (Figure 2A). In the NIR-PIT treated groups, quantitative evaluation of IR700 fluorescence intensity was performed with the %TBR based on pre-treatment TBR. IR700 fluorescence intensity in all the treated groups significantly decreased after the first exposure of NIR light (external exposure alone: 50 J/cm^2, interstitial exposure alone: 50 J/cm, combined exposure: 25 J/cm^2 + 25 J/cm) on day 0 and after the second exposure (external exposure alone: 100 J/cm^2, interstitial exposure alone: 100 J/cm, combined exposure: 50 J/cm^2 + 50 J/cm) on day 1 ($p < 0.0001$, paired t-test) (Figure 2B, Supplemental Figure 1B). In addition, IR700 fluorescence intensity immediately before the second exposure was higher than it was immediately after the first NIR exposure in all the treated groups ($p < 0.05$, paired t-test), which is likely due to wash in of fresh

conjugate into the treated region (Figure 2B, Supplemental Figure 1B). Time-course changes of pan-IR700 fluorescence intensity in NIR-PIT were similar among the 3 types of NIR light delivery methods (Supplemental Figure 1B-1D). IR700 fluorescence intensity immediately before the second exposure was significantly lower in the interstitial exposure alone group and in the combined exposure group than in the external exposure alone ($p < 0.05$, Tukey-Kramer test) (Supplemental Figure 1E). This finding suggests that interstitial exposure produces more effective photobleaching and/or photochemical reaction of the IR700, and this could be an indicator of its greater effectiveness in NIR-PIT.

Combination of external and interstitial light delivery in NIR-PIT produces superior tumor-killing

To investigate tumor-killing after NIR-PIT, BLI was performed before and after NIR-PIT up to day 6 (Figure 3A). BLI was quantitatively evaluated with the percent RLU on the formula; RLU Post/RLU Pre × 100 = %RLU. BLI is a highly sensitive tool for evaluating tumor cell viability after NIR-PIT and its intensity depends on the catalysis of luciferin by luciferase mediated by oxygen, Mg^{2+} and ATP [15]. In all the treated groups, %RLU greatly decreased immediately after NIR-PIT and then gradually increased (Figure 3B). This pattern of %RLU change is likely due to a large amount of

initial cell killing followed by slower regrowth of tumor cells. Post-treatment %RLU in external exposure alone, interstitial exposure alone, and combination with external and interstitial exposures were significantly lower at all time points after NIR-PIT than in the control group (n ≥ 8 mice in each group, $p < 0.0001$, Tukey-Kramer test) (Figure 3C). Among the 3 treated groups, interstitial exposure alone and the combined external/interstitial method showed significantly lower post-treatment %RLU compared to external exposure alone at 1, 4 and 5 days after NIR-PIT (n ≥ 9 mice in each group, $p < 0.05$, Tukey-Kramer test) and at 1, 3, 4 and 5 days after NIR-PIT, respectively (n ≥ 9 mice in each group, $p < 0.05$, Tukey-Kramer test) (Figure 3D). These data suggest that interstitial exposure alone and the combination of external and interstitial exposures induces superior *in vivo* tumor-killing effects compared to external exposure alone.

The combination of external/ interstitial light prolongs overall survival

All the NIR-PIT treated groups showed significantly decreases in tumor volume at all time points after NIR-PIT compared with controls ($p < 0.0001$, Tukey-Kramer test) and showed significantly prolonged survival ($p < 0.01$, Log-rank test), (Figure 4A, 4B). External/interstitial light delivery showed significantly greater tumor volume decreases compared to external exposure alone at 7, 10, 12, 14 and 17 days after NIR-PIT ($p < 0.05$, Tukey-Kramer test) (Figure 4A). On the other hand, there was no

significant difference in tumor volume decreases between external exposure alone and interstitial exposure alone, and between interstitial exposure alone and the combined exposure (Figure 4A). This suggests that the combination of external/interstitial exposures led to the slowest rate of tumor regrowth compared with the other NIR light exposure groups. Moreover, external/interstitial exposures had significantly prolonged survival after NIR-PIT compared with external exposure alone ($p = 0.0469 < 0.05$, Log-rank test) (Figure 4B). Taken together, our results suggest that the combination of external and interstitial exposures results in the most effective NIR light delivery among the 3 methods of NIR light delivery methods studied.

DISCUSSION

Previous studies have demonstrated that NIR-PIT is a highly specific and effective cancer treatment for tumors provided that NIR light can be readily delivered to the tumor [16–19]. Therefore, efficient NIR light delivery can enhance the therapeutic effects of NIR-PIT. The combination of external and interstitial NIR light delivery resulted in significantly less luciferase activity and reduced tumor volume compared to external exposure alone ($p < 0.05$). We hypothesize that the combination of light sources results in better coverage of the tumor than can be achieved with either approach alone.

This more homogeneous light dosimetry [1, 5–7], resulted in significantly better tumor cell killing and prolonged survival after NIR-PIT.

In this study, external/interstitial light exposure did not show significantly decreased fluorescence signal intensity in the tumor compared to external exposure alone. On the other hand, BLI demonstrated significant decreased signal intensity ($p < 0.05$). The fluorescence imaging reflects photobleaching and/or photochemical reactions of IR700 after NIR light exposure and is not directly related to tumor killing. BLI, however depends on viable cells with access to oxygen, energy and luciferin and more directly measures cytotoxicity. Therefore, BLI is more suitable for monitoring tumor viability after NIR-PIT than IR700 fluorescence imaging [20] although fluorescence imaging may have a role in documenting NIR light exposure within a tumor.

Interestingly, interstitial exposure alone also showed significantly decreased luciferase activity compared to external exposure alone ($p < 0.05$), yet there was no significant difference in tumor volume reduction or survival in these two groups. This suggests that the NIR light exposure from the optical fiber produces greater *in vivo* anti-tumor efficacy at least in the short term. However, over the longer-term our results suggest that external/interstitial light delivery results in more homogeneous light distribution producing superior therapeutic benefits. NIR light can transmit several

centimeters beneath the skin surface [8], yet irradiation from a single light source might produce heterogeneous NIR light exposure due to the presence of natural absorbers in the tissue, which in turn, could result in undertreated regions of the tumor. Homogeneous NIR light delivery with combined exposure at day 0 induces homogeneous delivery of APC in tumor bed due to NIR-PIT induced super-enhanced permeability and retention (SUPR) effects [21]. Therefore, second combined NIR light exposure at the day 1 could minimize survived tumor cells, resulted in suppressing tumor regrowth and improving long-term treatment outcome after NIR-PIT compared with external or interstitial exposure alone.

In the clinical trial of NIR-PIT in head and neck cancer patients, the combination of external and interstitial delivery of NIR light is the standard method of treatment. The results in the current study support the combination of external/interstitial exposures during NIR-PIT. In clinical practice, external exposure is rarely sufficient to treat all but the most superficial tumors. When the tumor is very small, externally applied light may be sufficient, but as the tumor grows the combination of light delivery methods appears to be necessary.

This study had several limitations. First, we used subcutaneously xenografted tumors and an orthotopic model might be considered more clinically-relevant [22, 23].

However, in the present study, it was important that a consistent size, shape and location of each tumor be maintained to enable a fair comparison of light delivery methods. The orthotopic model produces more variable results depending on how well the tumor is implanted within the organ. That is why we chose a simple subcutaneous xenograft tumor model. Second, both planar and linear light sources were used. This produces slightly unequal results for the external (planar) and interstitial (linear) light sources in terms of energy deposition as they use different units of measurement unit (J/cm^2 vs J/cm). In order to maintain approximately equivalent dosages of light we carefully adjusted the exposure time of the NIR light after simulation in order to deliver equal light doses to the tumors [13], but this limitation is difficult to avoid. Third, we performed NIR-PIT in mice bearing A431-luc tumor tumors of approximately 100 mm^3 in volume because smaller tumors were not fully established and larger tumor frequently contained large central necrosis. Therefore, the advantage of this combination exposure with both interstitial and external light was not validated for treating large tumors that are relevant to tumors in patients. However, considering that our data suggest homogeneous light exposure in treated tumors using multiple light sources is essential for performing effective NIR-PIT, a combined exposure would be also beneficial in treating large tumors. Finally, we monitored tumor viability after

NIR-PIT with BLI because a previous report has indicated that BLI evaluated therapeutic effects after NIR-PIT especially in acute phase [20], yet a luciferase expressing cell line has such a weak signal that it can only be detected by photon counting because it cannot form a good image. Since imaging methods of high sensitivity-high resolution with fluorescent proteins has been reported [24-28], further investigation is required for comparing luciferase photon counting with fluorescence imaging with fluorescent proteins in evaluation of tumor viability after NIR-PIT.

NIR-PIT differs from conventional photodynamic therapy (PDT) in several aspects. PDT produces substantially more toxicity due to non-specificity of photosensitizers which accumulates in tumor and non-tumor tissue as well. Light activation results in on-target and off-target damage resulting in dose-limiting toxicities. Porphyrin photosensitizers used in PDT do not selectively target cancer at the cellular level [29-31]. Precise control of laser irradiation during treatment is difficult to achieve resulting in damage to surrounding healthy organs and/or blood vessels. Recently, flexible coaxial laser endoscopes, which localize the laser illumination only to the selected tumor target, with minimal illumination of the surrounding tissue was reported [32-33]. While this improves the safety of PDT, there is still collateral damage on normal surrounding tissue. Moreover, after injection of modern porphyrin derivatives,

the patient remains systemically photosensitive for over a week [34]. In contrast, since a hydrophilic phthalocyanine-based photoabsorber, IR700, which does not have photosensitizing effects by itself, is used in NIR-PIT, the results are much more selective. No systemic photosensitivity is observed since the agent is only effective where it binds a sufficient number of target molecules on the cell membrane to cause damage [1]. Because of the highly selective binding of APC to cancer cells compared with normal cells, NIR light delivery does not have to be accurate as PDT. Additionally, Most PDT agents are activated by visible range light which penetrates only a few millimeters in tissue [35-36], whereas the NIR light used in NIR-PIT can penetrate up to two centimeters into tissue [13]. Finally, because NIR-PIT induces selective immunogenic cell death only in targeted cancer cells, it spares all the immune cells in the local tumor micro-environment in tumor beds [5]. Therefore, rapid and effective activation of anti-cancer host immunity is induced by NIR-PIT, whereas that effect is more muted in PDT.

In conclusion, the combination of external and interstitial NIR light sources yielded superior therapeutic efficacy compared to either delivery method alone. These findings comport with the ongoing Phase I/II study of NIR-PIT in head and neck cancers in which a combination of light delivery methods was successfully employed.

Although the combination of light delivery means that the procedure is more invasive, the improved tumor response more than justifies the relatively minimal procedure of placing interstitial catheters, which can be performed under local or general anesthesia. This study provides a rationale for the combined use of external/interstitial light sources in NIR-PIT.

ABBREVIATION

APC, antibody–photoabsorber conjugates; ATP, adenosine triphosphate; BLI, bioluminescence imaging; EGFR, epidermal growth factor receptor; FDA, Food and Drug Administration; HER1, human epidermal growth factor receptor 1; IR700, IRDye700DX; NIR, near infrared; pan-IR700, IR700-conjugated panitumumab; PIT, photoimmunotherapy; RLU, relative light units; ROI, regions of interest; SEM, standard error of the mean; TBR, target-to-background ratio

AUTHORS' CONTRIBUTIONS

Y.M. mainly designed and conducted experiments, performed analysis and wrote the manuscript; T.N., K.S., F.M. and S.O. performed analysis; P.L.C. wrote the manuscript and supervised the project; and H.K. planned and initiated the project,

designed and conducted experiments, wrote the manuscript, and supervised the entire project.

ACKNOWLEDGEMENTS

This research was supported by the Intramural Research Program of the National Institutes of Health, National Cancer Institute, Center for Cancer Research.

CONFLICTS OF INTEREST

The authors declare no conflicts of interest.

FUNDING

This research was supported by the Intramural Research Program of the National Institutes of Health, National Cancer Institute, Center for Cancer Research (ZIA BC 011513).

REFERENCES

(1) Mitsunaga, M.; Ogawa, M.; Kosaka, N.; Rosenblum, L. T.; Choyke, P. L.; Kobayashi, H. Cancer cell–selective *in vivo* near infrared photoimmunotherapy targeting specific membrane molecules. *Nat Med*. **2011**, 17 (12), 1685–1691.

(2) Willingham, M. C. Cytochemical methods for the detection of apoptosis. *J Histochem Cytochem.* **1999**, 47 (9), 1101–1109.

(3) Ziegler, U.; Groscurth, P. Morphological features of cell death. *News Physiol. Sci.* **2004**, 19, 124–128.

(4) Bezu, L.; Gomes-de-Silva, L. C.; Dewitte, H.; Breckpot, K.; Fucikova, J.; Spisek, R.; Galluzzi, L.; Kepp, O.; Kroemer, G. Combinatorial strategies for the induction of immunogenic cell death. *Front Immunol.* **2015**, 6: 187.

(5) Ogawa, M.; Tomita, Y.; Nakamura, Y.; Lee, M. J.; Lee, S.; Tomita, S.; Nagaya, T.; Sato, K.; Yamauchi, T.; Iwai, H., Kumar, A.; Haystead, T.; Shroff, H.; Choyke, P. L.; Trepel, J. B.; Kobayashi, H. Immunogenic cancer cell death selectively induced by near infrared photoimmunotherapy initiates host tumor immunity. *Oncotarget*. **2017**, 8 (6), 10425–10436.

(6) Mitsunaga, M.; Nakajima, T.; Sano, K.; Kramer-Marek, G.; Choyke, P. L.; Kobayashi, H. Immediate *in vivo* target-specific cancer cell death after near infrared photoimmunotherapy. *BMC Cancer.* **2012**, 12, 345

(7) Sato, K.; Nakajima, T.; Choyke, P. L.; Kobayashi H. Selective cell elimination in vitro and in vivo from tissues and tumors using antibodies conjugated with a near infrared phthalocyanine. *RSC Adv.* **2015**, 5 (32), 25105–25114.

(8) Dougherty, T. J.; Gomer, C. J.; Henderson, B. W.; Jori, G.; Kessel, D.; Korbelik, M.; Moan, J.; Peng, Q. Photodynamic therapy. *J Natl Cancer Inst.* **1998**, 90 (12), 889–905.

(9) Svanberg, K.; Bendsoe, N.; Axelsson, J.; Andersson-Engels, S.; Svanberg, S. Photodynamic therapy: superficial and interstitial illumination. *J Biomed Opt.* **2010**,15 (4), 041502.

(10) Patel, H.; Mick, R.; Finlay, J.; Zhu, T. C.; Rickter, E.; Cengel, K. A.; Malkowicz, S. B.; Hahn, S. M.; Busch, T. M. Motexafin lutetium-photodynamic therapy of prostate cancer: short- and long-term effects on prostate-specific antigen. *Clin Cancer Res.* **2008**, 14 (15), 4869–4876.

(11) Jerjes, W.; Upile, T.; Hamdoon, Z.; Abbas, S.; Akram, S.; Mosse, C. A.; Morley, S.; Hopper, C. Photodynamic therapy: The minimally invasive surgical intervention for advanced and/or recurrent tongue base carcinoma. *Lasers Surg Med.* **2011**, 43 (4), 283–292.

(12) Ortner, M. A. Photodynamic therapy for cholangiocarcinoma. *Lasers Surg Med.*

2011, 43 (7), 776–780.

(13) Okuyama, S.; Nagaya, T.; Nakamura, Y.; Sato, K.; Ogata, F.; Maruoka, Y.; Choyke, P. L.; Kobayashi, H. Interstitial near-infrared photoimmunotherapy: effective treatment areas and light doses needed for use with fiber optic diffusers. *Oncotarget.* **2018** [Epub ahead of print].

(14) Sato, K.; Watanabe, R.; Hanaoka, H.; Harada, T.; Nakajima, T.; Kim, I.; Paik, C. H.; Choyke, P. L.; Kobayashi, H. Photoimmunotherapy: comparative effectiveness of two monoclonal antibodies targeting the epidermal growth factor receptor. *Mol. Oncol.* **2014**, 8 (3), 620–632.

(15) Badr, C. E. Bioluminescence imaging: basics and practical limitations. *Methods Mol Biol.* **2014**, 1098, 1–18.

(16) Sato, K.; Nagaya, T.; Choyke, P. L.; Kobayashi, H. Near infrared photoimmunotherapy in the treatment of pleural disseminated SCLC: preclinical experience. *Theranostics.* **2015**, 5 (17), 698–709.

(17) Nagaya, T.; Nakamura, Y.; Sato, K.; Harada, T.; Choyke, P. L.; Hodge, J. W.; Schlom, J.; Kobayashi, H. Near infrared photoimmunotherapy with avelumab, an anti-programmed death-ligand 1 (PD-L1) antibody. *Oncotarget.* **2017**, 8 (5), 8807–8817.

(18) Nagaya, T.; Nakamura, Y.; Sato, K.; Zhang, Y. F.; Ni, M.; Choyke, P. L.; Ho, M.; Kobayashi, H. Near infrared photoimmunotherapy with an anti-mesothelin antibody. *Oncotarget.* **2016**, 7 (17), 23361–23369.

(19) Nakamura, Y.; Bernardo, M.; Nagaya, T.; Sato, K.; Harada, T.; Choyke, P. L.; Kobayashi, H. MR imaging biomarkers for evaluating therapeutic effects shortly after near infrared photoimmunotherapy. *Oncotarget.* **2016**, 7 (13), 17254–17264.

(20) Maruoka, Y.; Nagaya, T.; Nakamura, Y.; Sato, K.; Ogata, F.; Okuyama, S.; Choyke, P. L.; Kobayashi, H. Evaluation of early therapeutic effects after near-infrared photoimmunotherapy (NIR-PIT) using luciferase-luciferin photon-counting and fluorescence imaging. *Mol Pharm.* **2017**, 14 (12), 4628–4635.

(21) Sano, K.; Nakajima, T.; Choyke, P. L.; Kobayashi, H. Markedly enhanced permeability and retention effects induced by photo-immunotherapy of tumors. *ACS Nano.* **2013**, 7 (1), 717–724.

(22) Hoffman, R. M. Orthotopic metastatic mouse models for anticancer drug discovery and evaluation: a bridge to the clinic. *Invest New Drugs.* **1999**, 17 (4), 343–359.

(23) Hoffman, R. M. Patient-derived orthotopic xenografts: better mimic of metastasis than subcutaneous xenografts. *Nat Rev Cancer.* **2015**, 15 (8), 451–452.

(24) Hoffman, R. M. The multiple uses of fluorescent proteins to visualize cancer in

vivo. *Nat Rev Cancer*. **2005**, 5 (10), 796–806.

(25) Hoffman, R. M; Yang, M. Subcellular imaging in the live mouse. *Nat Protoc.* **2006**, 1 (2), 775–782.

(26) Hoffman, R. M; Yang, M. Color-coded fluorescence imaging of tumor-host interactions. *Nat Protoc.* **2006**, 1 (2), 928–935.

(27) Hoffman, R. M; Yang, M. Whole-body imaging with fluorescent proteins. *Nat Protoc.* **2006**, 1 (2), 775–782.

(28) Hoffman, R. M. Application of GFP imaging in cancer. *Lab Invest.* **2015,** 95 (4), 432–452.

(29) DeLaney, T. F.; Sindelar, W. F.; Tochner, Z.; Smith, P. D.; Friauf, W. S.; Thomas, G,; Dachowski, L.; Cole, J. W.; Steinberg, S. M.; Glatstein, E. Phase I study of debulking surgery and photodynamic therapy for disseminated intraperitoneal tumors. *Int J Radiat Oncol Biol Phys* **1993,** 25 (3), 445-457.

(30) Hino, H.; Murayama, Y.; Nakanishi, M.; Inoue, K.; Nakajima, M.; Otsuji, E. 5-Aminolevulinic acid-mediated photodynamic therapy using light-emitting diodes of different wavelengths in a mouse model of peritoneally disseminated gastric cancer. *J Surg Res* **2013.** 185(1), 119-126.

(31) Kishi, K.; Yano, M.; Inoue, M.; Miyashiro, I.; Motoori, M.; Tanaka, K.; Goto, K.;

Eguchi, H.; Noura, S.; Yamada, T.; Ohue, M.; Ohigashi, H.; Ishikawa, O. Talaporfin-mediated photodynamic therapy for peritoneal metastasis of gastric cancer in an in vivo mouse model: drug distribution and efficacy studies. *Int J Oncol* **2010.** 36(2), 313-320.

(32) Hu, Y.; Masamune, K. Flexible coaxial laser endoscope with arbitrarily selected spots in endoscopic view for photodynamic tumor therapy. *Appl Opt* **2016.** 55(30), 8433-8440.

(33) Hu, Y.; Masamune, K. Flexible laser endoscope for minimally invasive photodynamic diagnosis (PDD) and therapy (PDT) toward efficient tumor removal. *Opt Express* **2017.** 25(14), 16795-16812.

(34) Acerbi, F.; Broggi, M.; Eoli, M.; Anghileri, E.; Cuppini, L.; Pollo, B.; Schiariti, M.; Visintini, S.; Orsi, C.; Franzini, A.; Broggi, G.; Ferroli, P. Fluorescein-guided surgery for grade IV gliomas with a dedicated filter on the surgical microscope: preliminary results in 12 cases. *Acta Neurochir (Wien)* **2013.** 155(7), 1277-1286.

(35) Grant, W. E.; Speight, P. M.; Hopper, C.; Bown, S. G. Photodynamic therapy: an effective, but non-selective treatment for superficial cancers of the oral cavity. *Int J Cancer* **1997.** 71(6), 937-942.

(36) Kobayashi, W.; Liu, Q.; Nakagawa, H.; Sakaki, H.; The, B.; Matsumiya, T.;

Yoshida, H.; Imaizumi, T.; Satoh, K.; Kimura, H. Photodynamic therapy with mono-L-aspartyl chlorin e6 can cause necrosis of squamous cell carcinoma of tongue: experimental study on an animal model of nude mouse. *Oral Oncol* **2006.** 42(1), 46-50.

FIGURE LEGENDS

Figure 1. Overview of external and interstitial light exposure in NIR-PIT. A. A NIR laser system (BWF5-690-8-600-0.37; B & W TEK INC., Newark, DE, USA) was used in this study. **B.** A laser beam irradiator with 10 mm diameter was used as a light source for external light exposure. **C.** A 0.98 mm diameter cylindrical diffusing fiber with 30 mm irradiation length was used as a light source for interstitial light exposure. **D.** The scheme explaining external and interstitial light exposures to the tumor bed as NIR light delivery methods**.** External light exposure was performed by NIR light irradiation from above a subcutaneously xenografted tumor in A431-luc tumor-bearing mice. Interstitial light exposure of NIR light was performed after the cylindrical diffusing fiber was percutaneously inserted just under the targeted tumor with an 18G needle with a translucent catheter. The light dose administered in external and interstitial light exposure was respectively determined based on the surface area per unit (J/cm^2) and based on the length per unit (J/cm) because light sources used in external and interstitial light exposure are planar sources and linear sources, respectively.

Figure 2. IR700 fluorescence real-time imaging before and after NIR light exposure in PIT. A. Schema of NIR-PIT. IR700 fluorescence images were scanned at

each time point as shown. **B.** IR700 fluorescence real-time images of A431-luc tumor bearing mice. Yellow arrows indicate the tumor. In all NIR-PIT treated groups, IR700 fluorescence intensities greatly decreased immediately after the first exposure of NIR light on day 0 and immediately after the second irradiation on day 1. Additionally, IR700 fluorescence intensities before the second irradiation on day 1 were significantly higher than those immediately after the first irradiation on day 0 in the treated groups.

Figure 3. Bioluminescence imaging in response to NIR-PIT. A. Schema of imaging. Bioluminescence images were scanned at each time point as shown. **B.** Bioluminescence real-time images of A431-luc tumor bearing mice for NIR-PIT. In all treated groups, the signal intensities significantly decreased 1 day after each NIR light exposure and gradually increased due to tumor regrowth. **C.** Quantitative analysis of luciferase activity before and after NIR-PIT in A431-luc tumor bearing mice. %RLU in all the NIR-PIT treated groups showed significant decreases at all time points after NIR-PIT compared to the control group ($n \geq 8$ mice in each group; $*p < 0.01$, vs. control group, Tukey-Kramer test). **D.** Comparison of luciferase activity among all the NIR-PIT treated groups. Combination with external/interstitial light showed significantly lower %RLU compared to external exposure alone on day 1, 3, 4 and 5 (n

≥ 9 mice in each group; *p < 0.05, vs. combined exposure, Tukey-Kramer test). Interstitial exposure alone showed significantly lower %RLU compared to external exposure alone on day 1, 4 and 5 (n ≥ 9 mice in each group; **p < 0.05, vs. interstitial exposure alone, Tukey-Kramer test).

Figure 4. Tumor growth inhibition by NIR-PIT and long-term observation after NIR-PIT. A. All the NIR-PIT treated groups showed significantly reduced tumor volume after NIR-PIT at all time points (n ≥ 8 mice in each group; ***p < 0.0001, vs. the other groups, Tukey-Kramer test), compared to the control group. Combination with external and interstitial light led to significantly reduced tumor volume in comparison with external exposure alone 7 days after NIR-PIT or later (n ≥ 8 mice in each group; *p < 0.05, **p < 0.01, vs. combined exposure, Tukey-Kramer test). **B.** All the NIR-PIT treated groups showed significantly prolonged survival (n ≥ 8 mice in each group; **p < 0.01, Log-rank test), compared to the control group. Combination with external and interstitial exposures in NIR-PIT led to significantly prolonged survival, compared to external exposure alone (n ≥ 8 mice in each group; *p < 0.05, Log-rank test).

Supplementary Figure 1. Changes of IR700 fluorescence intensity after NIR light

exposure in NIR-PIT. A. IR700 fluorescence images were scanned at each time point as shown. **B, C, D.** Time-course analysis of IR700 fluorescence intensity changes in all the NIR-PIT treated groups. All the NIR-PIT-treated groups respectively showed significant decrease in IR700 fluorescence intensity after the first exposure on day 0 and after the second exposure on day 1, compared to IR700 fluorescence intensity immediately before respective exposure (*$p < 0.0001$, vs. before PIT, paired *t*-test; ***$p < 0.0001$, vs. before the second exposure, paired *t*-test). Additionally, in all the treated groups, IR700 fluorescence intensity immediately before the second exposure was significantly higher than that immediately after the first exposure (**$p < 0.05$, vs. after the first exposure, paired *t*-test). **E.** Comparison of IR700 fluorescence before and NIR light exposure intensity among all the NIR-PIT treated groups. Interstitial exposure alone and combination with external and interstitial exposures showed significantly lower intensity immediately before the second exposure compared to external exposure alone, respectively (*$p < 0.05$, vs. external exposure alone, Tukey-Kramer test).

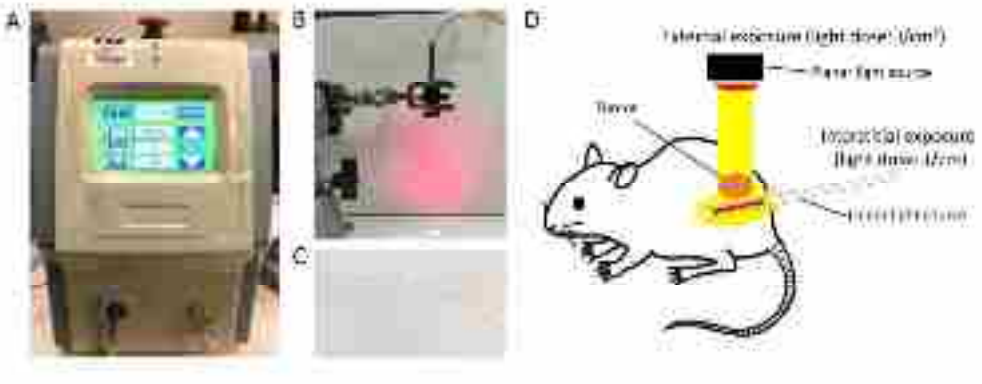

Figure 1. Overview of external and interstitial light exposure in NIR-PIT. A. A NIR laser system (BWF5-690-8-600-0.37; B & W TEK INC., Newark, DE, USA) was used in this study. B. A laser beam irradiator with 10 mm diameter was used as a light source for external light exposure. C. A 0.98 mm diameter cylindrical diffusing fiber with 30 mm irradiation length was used as a light source for interstitial light exposure. D. The scheme explaining external and interstitial light exposures to the tumor bed as NIR light delivery methods. External light exposure was performed by NIR light irradiation from above a subcutaneously xenografted tumor in A431-luc tumor-bearing mice. Interstitial light exposure of NIR light was performed after the cylindrical diffusing fiber was percutaneously inserted just under the targeted tumor with an 18G needle with a translucent catheter. The light dose administered in external and interstitial light exposure was respectively determined based on the surface area per unit (J/cm2) and based on the length per unit (J/cm) because light sources used in external and interstitial light exposure are planar sources and linear sources, respectively.

1329x536mm (96 x 96 DPI)

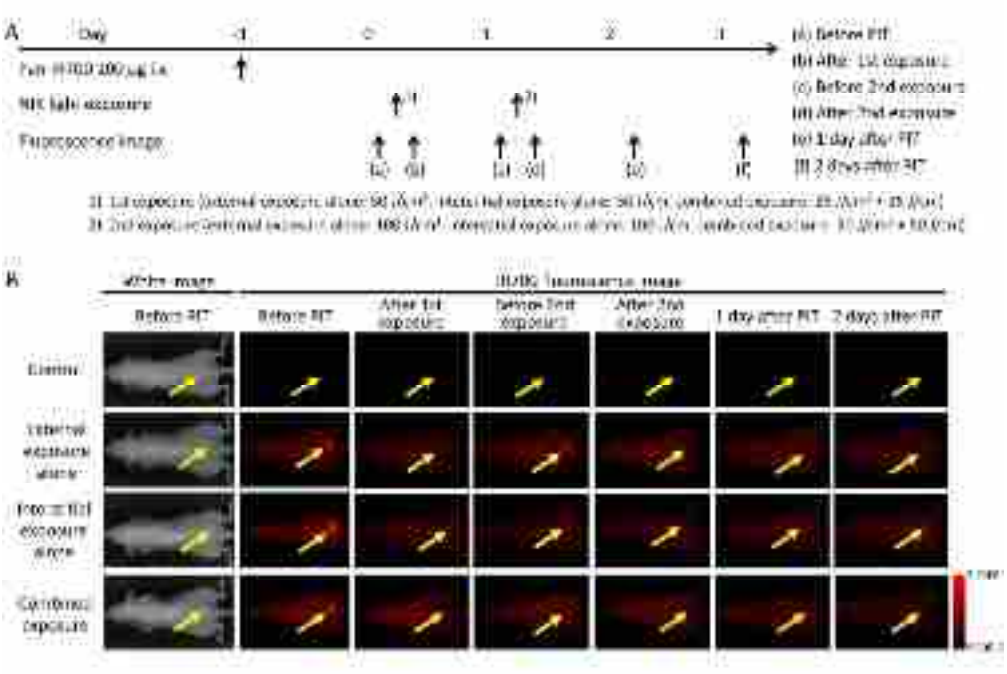

Figure 2. IR700 fluorescence real-time imaging before and after NIR light exposure in PIT. A. Schema of NIR-PIT. IR700 fluorescence images were scanned at each time point as shown. B. IR700 fluorescence real-time images of A431-luc tumor bearing mice. Yellow arrows indicate the tumor. In all NIR-PIT treated groups, IR700 fluorescence intensities greatly decreased immediately after the first exposure of NIR light on day 0 and immediately after the second irradiation on day 1. Additionally, IR700 fluorescence intensities before the second irradiation on day 1 were significantly higher than those immediately after the first irradiation on day 0 in the treated groups.

1422x967mm (96 x 96 DPI)

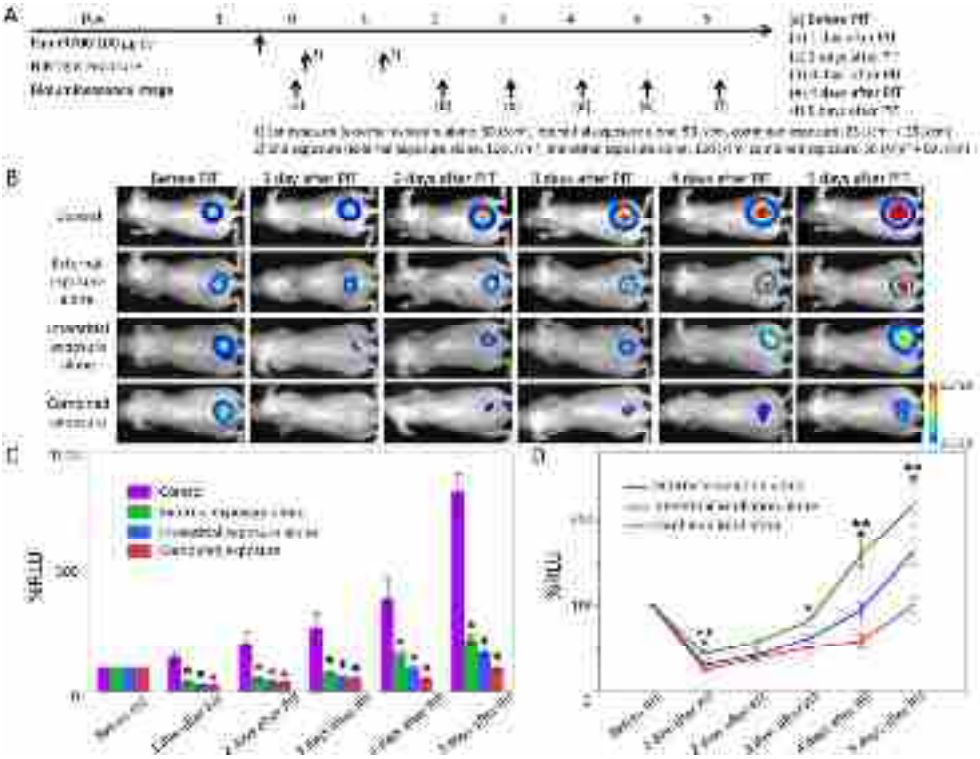

Figure 3. Bioluminescence imaging in response to NIR-PIT. A. Schema of imaging. Bioluminescence images were scanned at each time point as shown. B. Bioluminescence real-time images of A431-luc tumor bearing mice for NIR-PIT. In all treated groups, the signal intensities significantly decreased 1 day after each NIR light exposure and gradually increased due to tumor regrowth. C. Quantitative analysis of luciferase activity before and after NIR-PIT in A431-luc tumor bearing mice. %RLU in all the NIR-PIT treated groups showed significant decreases at all time points after NIR-PIT compared to the control group (n ≥ 8 mice in each group; *p < 0.01, vs. control group, Tukey-Kramer test). D. Comparison of luciferase activity among all the NIR-PIT treated groups. Combination with external/interstitial light showed significantly lower %RLU compared to external exposure alone on day 1, 3, 4 and 5 (n ≥ 9 mice in each group; *p < 0.05, vs. combined exposure, Tukey-Kramer test). Interstitial exposure alone showed significantly lower %RLU compared to external exposure alone on day 1, 4 and 5 (n ≥ 9 mice in each group; **p < 0.05, vs. interstitial exposure alone, Tukey-Kramer test).

1422x1066mm (96 x 96 DPI)

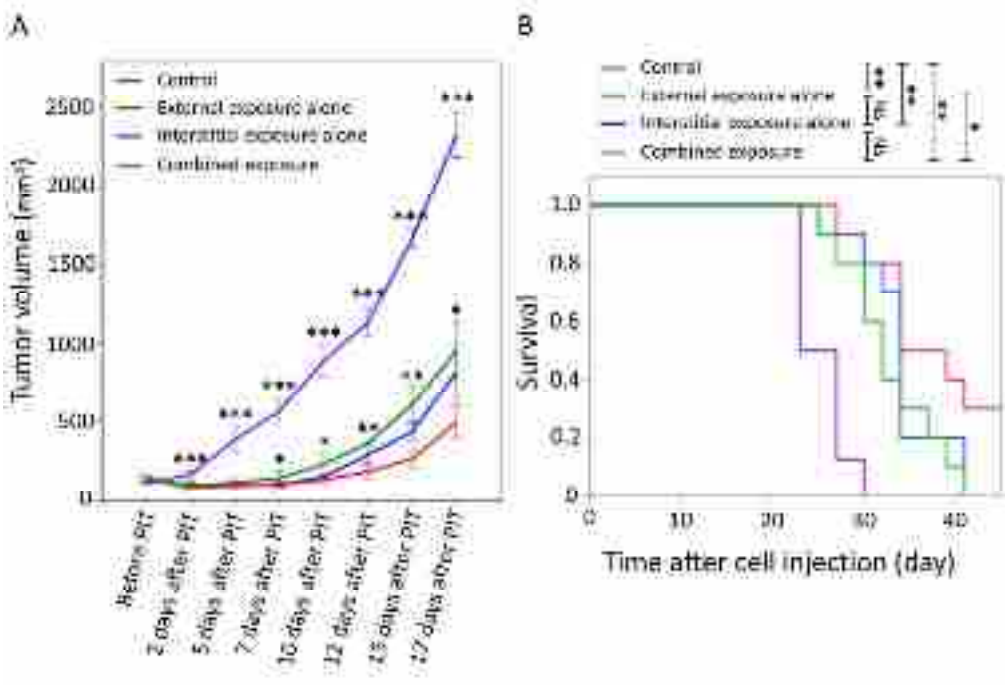

Figure 4. Tumor growth inhibition by NIR-PIT and long-term observation after NIR-PIT. A. All the NIR-PIT treated groups showed significantly reduced tumor volume after NIR-PIT at all time points (n ≥ 8 mice in each group; ***p < 0.0001, vs. the other groups, Tukey-Kramer test), compared to the control group. Combination with external and interstitial light led to significantly reduced tumor volume in comparison with external exposure alone 7 days after NIR-PIT or later (n ≥ 8 mice in each group; *p < 0.05, **p < 0.01, vs. combined exposure, Tukey-Kramer test). B. All the NIR-PIT treated groups showed significantly prolonged survival (n ≥ 8 mice in each group; **p < 0.01, Log-rank test), compared to the control group. Combination with external and interstitial exposures in NIR-PIT led to significantly prolonged survival, compared to external exposure alone (n ≥ 8 mice in each group; *p < 0.05, Log-rank test).

1422x982mm (96 x 96 DPI)